Oriented Internal Electrostatic Fields Cooperatively Promote Ground & Excited State Reactivity: A Case Study in Photochemical CO_2 Capture

Mitchell T. Blyth, Benjamin B. Noble, Isabella C. Russell, Michelle L. Coote*

ARC Centre of Excellence for Electromaterials Science, Research School of Chemistry, Australian National University, Canberra, Australian Capital Territory, 2601, Australia

**Corresponding Author email michelle.coote@anu.edu.au*

ABSTRACT:

Oriented electrostatic fields can exert catalytic effects upon both the kinetics and thermodynamics of chemical reactions; however, the vast majority of studies thus far have focused upon ground state chemistry and rarely consider any more than a single class of reaction. In the present study, we first use density functional theory (DFT) calculations to clarify the mechanism of CO_2 storage *via* photochemical carboxylation of *o*-alkylphenyl ketones, originally proposed by Murakami *et al*. (J. Am. Chem. Soc. 2015, 137, 14063); we then demonstrate that oriented internal electrostatic fields arising from remote charged functional groups (CFGs) can selectively and cooperatively promote both ground- and excited-state chemical reactivity at all points along the revised mechanism, in a manner otherwise difficult to access *via* classical substituent effects. What is particularly striking is that electrostatic field effects upon key photochemical transitions are *predictably enhanced* in increasingly polar solvent, thus overcoming a central limitation of the electrostatic catalysis paradigm. We explain these observations, which should be readily extendable to the ground state.

INTRODUCTION

The understanding that oriented electrostatic fields (OEFs) can be used to catalyse and control the reactivity or selectivity of chemical reactions has recently sparked immense interest from both the theoretical[1–6] and experimental[7–11] community. In part, this interest is motivated by the ubiquity and effectiveness of OEFs within the active sites of enzymes[12,13] and an increasing awareness of unrecognized or under-utilized electrostatic field effects within organic chemistry.[14–17] Additionally, the use of OEFs within organic chemistry proposes numerous advantages, of which the most pertinent include their orthogonality to existing approaches (i.e. light, heat, co-catalysts) and their strong directionality. However, the adoption of OEFs into common procedure is limited in part by the attenuation of their effects in polar solvents, and limited information about their effects in complex multi-step mechanisms. Herein, we attempt to simultaneously address both of these concerns.

We have previously found that OEFs arising from charged functional groups (CFGs) are able to selectively modify key photochemical transitions in Type I photoinitiators,[18,19] and demonstrated that OEFs can favourably affect the rates, regio- and diastereoselectivity of Diels-Alder reactions.[20,21] We were thus motivated to identify some mechanism which featured both components, and determine if the effects of OEFs were synergistic and synthetically useful in a complex yet realistic model system.

Recently, Murakami and co-workers[22] demonstrated that irradiation of *o*-alkyl aromatic ketones could achieve photochemical CO_2 capture and storage under mild conditions; effectively using UV light to drive an endergonic transformation (**Scheme 1A**). In their original report, Murakami and co-workers suggested on the basis of preliminary DFT calculations that the mechanism of CO_2 capture was consistent with a typical photoenolization/Diels-Alder (PEDA) sequence, as exemplified in **Scheme 1B**. Such sequences were first established by Yang and Rivas[23] in 1961, and have since been the subject of intense scrutiny.

Under Murakami's PEDA mechanism, absorption of light by the *o*-alkylphenyl ketone **1** generates a singlet excited state **S_1-B**, which decays *via* intersystem crossing (ISC) to the corresponding triplet, **T_1-B**. A Norrish Type II reaction forms the transient *o*-quinodimethane (*Z*)-**C** on the triplet surface, which exists in fast equilibrium with (*E*)-**C**. Either isomer can undergo ISC to yield the corresponding singlet dienol (*Z*)-**A** or (*E*)-**A**, whereupon the latter may

be trapped *via* subsequent Diels-Alder cycloaddition (in this case, with CO_2) to afford the enol-lactone **2**, which rearranges into the observed keto-carboxylic acid **3**. The (*Z*)-**A** dienol rapidly undergoes 1,5-sigmatropic hydrogen atom transfer on the singlet surface to regenerate the starting material, whereas the reketonization of (E)-**A** requires an intermolecular proton transfer and is relatively slow. Thus, to drive the reaction forward, isomerization from (Z)-**A** to (E)-**A** must occur on the triplet surface, such that the latter becomes kinetically trapped following ISC.

While this PEDA mechanism appears to satisfactorily explain the process developed by Murakami and co-workers, a subsequent theoretical study by Su and Su[24] proposed an alternative. In particular, the (*E*)-(*Z*) isomerization was ignored and it was instead proposed that CO_2 addition occurs directly to the (*Z*)-isomer *via* an 8-membered transition state, directly affording the keto-carboxylic acid **3** without generating the enol-lactone **2** (**Scheme 1C**). However, based on the calculations presented in that work, there was a large barrier for the CO_2 addition (65 kJ mol^{-1} on a relative scale) in competition with a much smaller barrier (38 kJ mol^{-1}) for hydrogen transfer to regenerate the starting material. That is, under this mechanism, the starting alkylphenylketone reforms five orders of magnitude faster than the product. Even allowing for the potential uncertainty in the DFT calculations, this is difficult to reconcile with the experimental results.

In the present work we first aim to clarify the mechanism of photochemical CO_2 storage by comparing on equal grounds the PEDA mechanism proposed by Murakami and co-workers with the mechanism of Su and Su. We then explore the effects of CFGs upon the full PEDA sequence, with the aim to harness OEFs to simultaneously drive photochemical and excited state reactivity while improving the competition between the (*E*)-(*Z*) isomerization and Diels-Alder cycloaddition pathways on the singlet surface.

COMPUTATIONAL METHODS

All calculations were performed using the Gaussian 16 electronic structure package.[25] Theoretical procedures were chosen based on our previous studies of related excited state reactions[18,26] and of electrostatic effects upon Diels-Alder reactions.[8,20,21] Geometries were optimized with the M06-2X[27] exchange correlation functional with the 6-31+G(d,p) basis set; time-dependent DFT (TD-DFT) calculations of excited states were performed at the same level of theory. Solvent corrections were obtained with the SMD continuum solvent model,[28] and the thermocycle approach was employed to determine Gibbs free energies in solution.[29] All energies given are from the conformationally searched, global minimum energy structures in both gas and solvent phases, unless otherwise indicated. Stability analysis was employed to approximately locate conical intersection points. Intrinsic reaction coordinate (IRC) calculations were used to verify the nature and connectivity of key transition states. Photochemical switches are calculated as a Boltzmann-weighted average from rotations about the CFG linker, with weights determined from the Gibbs free energies in solution. Point charge approximations and σ-induction controls were performed as in our previous studies.[18,30]

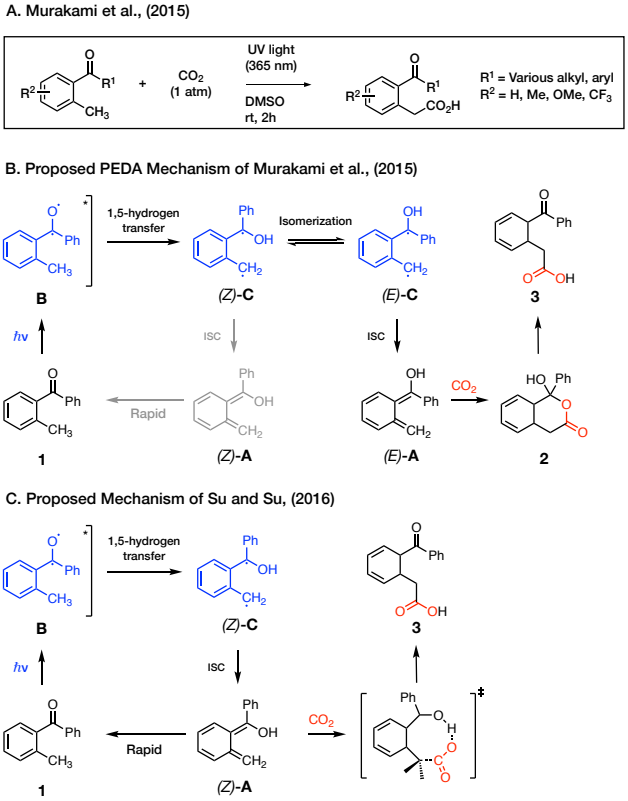

Scheme 1. Alternative proposed mechanisms for carboxylation of *o*-alkylphenyl ketones.[22,24]

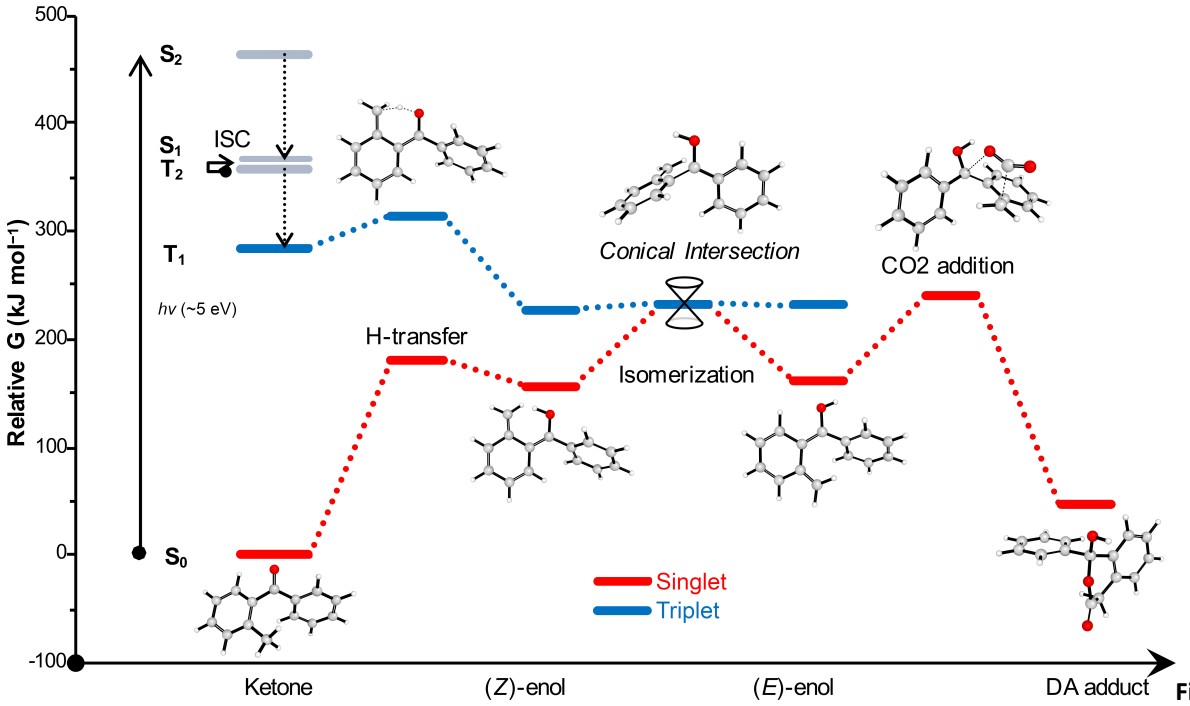

Figure 1. Computed Gibbs free energy surface (kJ mol^{-1}; 298 K; SMD DMSO) for Murakami's PEDA mechanism (**Scheme 1B**).

RESULTS AND DISCUSSION

Reaction Mechanism. The computed Gibbs free energy surface for photochemical carboxylation based on Murakami's PEDA mechanism (*vide supra*) is presented in **Figure 1**. Our results support the notion that hydrogen-transfer to form the *o*-quinodimethane must occur in the triplet state; this is followed by intersystem crossing at the conical intersection point of (*E*)-(*Z*) isomerisation to form the singlet (*E*)- or (*Z*)-dienol. On the singlet surface, the barrier for hydrogen atom transfer (HAT) from the (Z)-enol is substantially lower than on the triplet surface (24 kJ mol^{-1} versus 87 kJ mol^{-1} in DMSO, respectively), resulting in swift deactivation to the starting ketone. If, however, the (*E*)-enol is formed, it must first overcome the isomerisation barrier before deactivation can occur. While this is plausible, product formation is also possible because the barrier for isomerisation (68 kJ mol^{-1}) and for cycloaddition of CO_2 (78 kJ mol^{-1}) are close. Indeed, with the inclusion of one and two explicit solvent molecules, the two barriers are effectively degenerate, at between approximately 50 kJ mol^{-1} and 53 kJ mol^{-1}, respectively (Appendix §1).

In contrast, competition between CO_2 addition *via* Su and Su's mechanism[24] (83 kJ mol^{-1} at our level of theory) and HAT (24 kJ mol^{-1}) are such that deactivation is dominant. At their chosen level of theory, Su and Su report a more favourable barrier difference of 27 kJ mol^{-1} (in favour of HAT), however they fail to account for solvation effects, which are particularly significant given the initial phase difference between the (*Z*)-enol and CO_2. Moreover, the 8-membered transition state proposed by Su and Su is not supported by their own calculations; IRC calculations on their reported geometry at either their chosen level of theory or our own reveal that their transition state is merely an asynchronous Diels-Alder cycloaddition (Appendix §2). While Su and Su initially propose that cycloaddition occurs to the (*Z*)-enol, they erroneously report the geometry of the (*E*)-enol transition state in its place on two separate occasions, with no explanation as to how the (*E*)-enol might have formed. Summarising, if CO_2 addition were to occur to the (Z)-enol, it cannot occur in the manner suggested by Su and Su, and deactivation remains the dominant pathway, (irrespective of the excess internal energy remaining after relaxation from the Frank-Condon point to the triplet minimum); if CO_2 addition occurs to the (*E*)-enol, then their mechanism fails to consider the necessary isomerization.

Only Murakami's mechanism (**Scheme 1B, Figure 1**) can thus account for product formation. Based on this mechanism, the photochemical activation is governed by the feasibility of the S_0 to T_1 transition, while the efficiency of product formation is governed by the rate of HAT on the triplet surface and the competition between (*E*)-(*Z*) isomerization and CO_2 cycloaddition to the (*E*)-enol on

the singlet surface. We now explore the effect of charged functional groups on each of these processes.

Diels-Alder versus Isomerization. On the basis of the mechanistic insights provided by the previous section, we first turn to electrostatic control of the competition between (*E*)-(*Z*) isomerization and Diels-Alder cycloaddition, with an understanding that changes to this competition will likely have the greatest impact upon the rate of product formation. Due to pioneering work by Shaik and co-workers,[31] the effect of electrostatic fields upon the Diels-Alder reaction is now relatively well-understood; the transition state of an archetypal normal electron demand Diels-Alder reaction between an electron-rich diene such as an *o*-alkylphenylketone and an electron-poor dienophile such as CO_2 contains a significant degree of charge-transfer character. This character arises as a result of single electron transfer from the diene to the dienophile, which imparts the latter with a transient negative charge which is greatest in the transition state; electrostatically stabilising this transient charge amounts to electrostatic catalysis of the Diels-Alder reaction. However, the effect of electrostatic fields upon (*E*)-(*Z*) isomerization remains to be studied.[32]

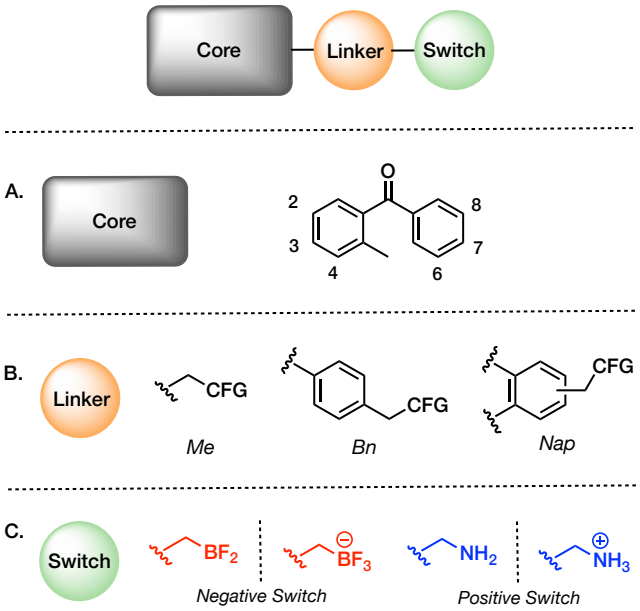

Scheme 2. The core *o*-alkylphenyl ketone motif (A), with indicated positions R2 to R8 bearing linkers *Me* through *Nap* (B) carrying charged functional group pairs (CFGs; C)

To identify the factors which drive selective electrostatic catalysis of either the Diels-Alder reaction or the (*E*)-(*Z*) isomerization process, we placed CFGs in both their anionic/cationic and neutral forms around the *o*-alkylphenylketone motif (**Scheme 2**). The model BF_2/BF_3^- pair was chosen to replace the more common $COOH/COO^-$ pair (to remove the risk of triplet decarboxylation), while the corresponding positive charge was modelled with the NH_2/NH_3^+ pair. Each pair was covalently attached to the *o*-alkylphenylketone motif by linkers of varied length, which we denote *Me*, *Bn*, and *Nap* respectively. Although the core conjugated motif changes with each of these linkers, concomitant changes to (1) molecular polarizability and (2) the distance and angle between the charge and affected dipoles permits direct comparison between realistic model systems across (3) a range of solvents in both the ground and excited state manifold, and the elucidation of the role these three factors play in cooperative electrostatic catalysis. Each CFG is not π-conjugated to the core motif, which helps to isolate electrostatic contributions; this is supported by point-charge calculations and σ-induction controls (Appendix §3, §4 of the Supporting Information).

The effects of forming cationic or anionic charges upon the relative barrier heights of (*E*)-(*Z*) isomerization and Diels-Alder cycloaddition as a function of substituent position are illustrated in **Figure 2,** (the uncharged partners to either switch have negligible effect upon the two barriers). We observe the greatest electrostatic effects when the CFG is spatially close to the intended reaction centre, the sign of the effect typically depends only on the sign of the applied field, and the effect is attenuated in polar solvent (Appendix §5). With a cationic CFG, we observe switches of up to 63 kJ mol^{-1} in favour of Diels-Alder cycloaddition (**Figure 2A**, position R4), or 49 kJ mol^{-1} in favour of (*E*)-(*Z*) isomerization (**Figure 2A**, position R7). Using an anionic CFG, we observe switches of up to 57 kJ mol^{-1} in favour of Diels-Alder cycloaddition (**Figure 2A**, position R7), or 13 kJ mol^{-1} in favour of (E)-(Z) isomerization (**Figure 2B**, position R4). The effects of OEFs upon individual barriers to either Diels-Alder cycloaddition or isomerization can exceed the change in relative barrier heights reported in **Figure 2**.

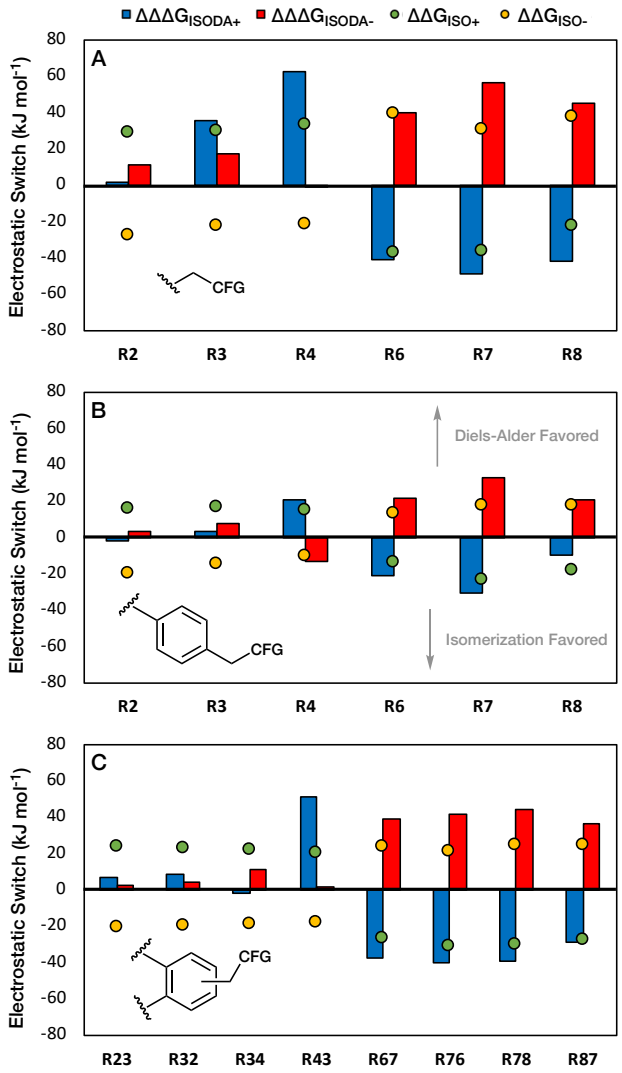

Figure 2. Electrostatic switches ($\Delta\Delta\Delta G_{ISODA}$; kJ mol^{-1}; 298 K; Gas) on the relative barrier heights of (*E*)-(*Z*) isomerization and Diels-Alder cycloaddition upon the introduction of cationic (blue) or anionic (red) charges as a function of substituent position for each of (**A**) *Me*, (**B**) *Bn*, and (**C**) *Nap* linkers. Switches ($\Delta\Delta\Delta G_{ISODA}$) are defined (Appendix S5) such that a positive or negative value implies that the Diels-Alder or isomerization pathway is favored, respectively. The change in barrier to isomerization ($\Delta\Delta G_{ISO}$) upon introduction of cationic (green) or anionic (yellow) CFGs is strongly correlated with the $\Delta\Delta\Delta G_{ISODA}$ value, (Appendix S6), where a negative value of $\Delta\Delta G_{ISO}$ implies that isomerization is more favorable in the presence of the charge. Solvent effects are explored in the Supplementary Information and consistent with the results reported here (Appendix §5).

Significantly, we find that the magnitude and sign of the switches presented in **Figure 2** are more strongly linearly correlated with the change in barrier to (E)-(Z) isomerization (R^2=0.64) than with the corresponding change in barrier to cycloaddition (R^2=0.32; Appendix S6). After consideration, this is not surprising; we[20,21] and others[31] have previously demonstrated that electrostatic catalysis of the Diels-Alder reaction depends strongly upon the relative orientation of the applied field with respect to the bond-forming axis from the incoming dienophile (the "reaction-axis rule"), which in this case is orthogonal to the plane of the ring system to which the CFG is attached and therefore unlikely to have any *catalytic* effect (**Scheme 3B**).

In contrast, in the case of isomerization the applied OEF is largely co-planar with the rotating alkene bond, and its effect is determined by its sign and orientation with respect to the transition state dipole moment (**Scheme 3A**). The field promotes zwitterionic character in the isomerization transition state, which is in part responsible for the dipole direction illustrated in **Scheme 3A**.[32] This further explains why the magnitude and sign of the electrostatic switch appears strongly related to the choice of ring system, which is particularly clear when comparing the effect of a cationic CFG in positions R2-R4 versus positions R6-R8 in **Figure 2A-B** (and the corresponding positions in **2C**), and to a lesser extent the effect of an anionic CFG in those same positions. We additionally demonstrate that the changes in relative barrier heights are induced by charge (R^2=0.90), and effectively uncorrelated with the presence of an uncharged CFG (R^2=0.0013). The ability to induce such significant electrostatic switches on (E)-(Z) bond isomerization has broader implications for pH-responsive materials design.

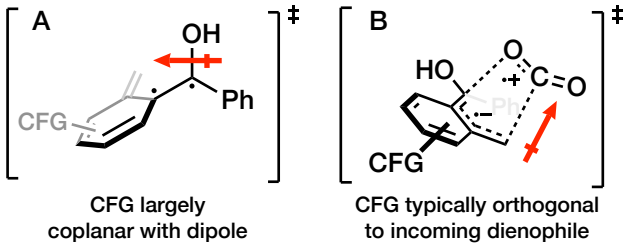

Scheme 3. The CFG-stabilized transition state dipole moments of the Diels-Alder (**A**) and (E)-(Z) isomerization (**B**) reactions, illustrating the origin of both the position-dependence and relative magnitudes of the observed electrostatic switches in **Figure 2**. Dipoles are defined from negative to positive, in Debye.

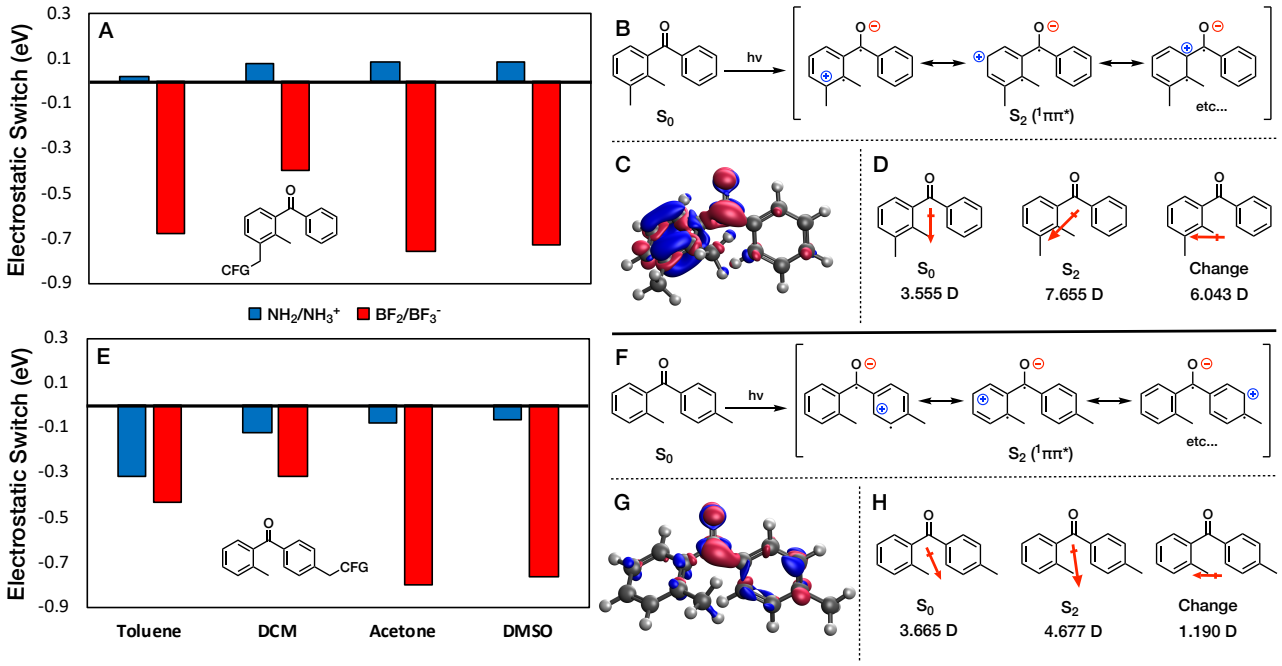

Figure 3. The effect of *Me*-linked electrostatic fields arising from cationic (blue) and anionic (red) CFGs in positions R4 (**A**) and R7 (**E**) upon the $^1\pi\pi^*$ transition of the *o*-alkylphenyl ketone motif, in increasingly polar solvents. Selected delocalisation contributors to the non-adiabatic S_2 state with CFGs removed (**B**, **F**) indicate cationic character at positions R2 and R4 in **A** and polarizable character in **E**, which is shown by density analysis (decreased S_2 density in blue; increased in red; consistent isovalue chosen aesthetically), to result in a large vertical transition dipole (**D**, **H**) in **A**. Under the charge-dipole model, stabilizing this dipole is predicted to red-shift the transition to an extent that is attenuated in polar solvent. That large switches remain for **E** in polar solvent suggests that polarizability dominates, and is stabilised, in polar solvent. Dipoles are defined from negative to positive, in Debye; out-of-plane dipole component changes are negligible. Switches are defined as the difference between the charged and neutral systems; a negative value indicates stabilization of the transition due to charge.

Effect of CFGs on the ππ* excited state and the role of polarizability. In ground-state chemistry, electrostatic field effects have been generally well approximated by a simple charge-dipole model, where the magnitude of the (de)stabilization depends on the separation between the charge and the affected dipole, the magnitude of the dipole, and its relative orientation, as well as the solvent polarity.[2,3] However, polarization can also play a key role in enhancing stabilization effects and diminishing destabilization,[30,33] particularly in resonance stabilized systems. In our recent study of Type I photoinitiators,[18] we found that polarization effects were particularly large in ππ* excited states, to the extent that stabilization exceeded 1 eV, while destabilizing effects diminished to almost zero.

On the basis of results from the previous section (**Figure 2**), our analysis of co-operative field effects upon excited states and photochemical transitions will focus on CFGs at positions R4 and R7 as these are good candidates for driving the competition between isomerization and cycloaddition in favour of the latter. In particular, we wish to understand how these effects change as a function of (1) the sign and position of the applied field, (2) the identity of the linker and the role of polarizability, and (3) the polarity of the solvent medium. For tractability, we initially restrict our consideration of electrostatic field effects upon photochemical transitions to the $^1\pi\pi^*$ state with a *Me* linker, which is typically most affected and most relevant. Field effects at the remaining positions and upon other relevant transitions are beyond the scope of the present work, but the complete dataset and preliminary analysis of the three aforementioned factors (averaged over substituent position) are provided in the Supplementary Information (Appendix §6), and consistent with the general insights presented here.

Figure 3 shows the effect of cationic and anionic CFGs on the solution-phase energies of the $^1\pi\pi^*$ transition of the *Me*-linked *o*-alkylphenyl ketone motif. It is immediately clear that the effects of positive and negative charges are largely unequal in magnitude and opposite in sign. A cationic CFG at R4 and R7 is weakly (de)stabilising, respectively, and an anionic CFG in position R4 is strongly stabilising (between 0.40 eV to 0.76 eV), consistent with the charge-dipole model presented in **Figure 3**. Under this

model, cationic and anionic charges at R4 should (de)stabilise the non-adiabatic $S_0 \rightarrow S_2$ transition dipole, respectively, and *vice-versa* at R7.

However, an anionic CFG at position R7 is also found to be stabilizing, and the magnitude of stabilization is initially attenuated—and then enhanced—in increasingly polar solvent, irrespective of position, in apparent disregard for a central limitation of electrostatic catalysis; this phenomenon was first theorized for the singlet excited states of olefin isomerization in the 1970s.[34] In fact, only the effects of the cationic CFG are consistent with the charge-dipole model. In contrast, the effects of an anionic CFG are dominated by molecular polarizability induced by the anion, which results in the observed unequal magnitude and supposedly position-invariant field effects of the latter (Appendix §6).

A novel consequence of this polarizability regime is that the observed electrostatic switching is related to the relative change in amount and stability of *any* charge-separated character in the excited state (relative to the ground state), and not merely the stabilisation of the resulting net transition dipole (though this is still pertinent, compare the effects of a negative charge in toluene at positions R4 and R7). For example, in **Figure 3** we observe a crossover point between DCM and acetone, in which the polarization induced by the *Me*-linked anionic CFG is first stabilized only by the charge and accordingly attenuated from toluene to DCM, and then co-operatively stabilized by both the charge and surrounding solvent in acetone and DMSO. We further demonstrate using the *Bn*- and *Nap*-linked systems (Appendix §7) that by controlling the extent of change in charge-separated character throughout the $S_0 \rightarrow S_2$ transition, one can predictably enhance or diminish solvent attenuation of electrostatic effects. We envisage that this principle can be generalised to overcome solvent attenuation in the ground state for certain classes of molecule and work is ongoing in this direction.

Cooperative Ground and Excited State Control. Returning to the aim of this study, we have now demonstrated that electrostatic fields arising from CFGs can have a significant effect upon both photochemical absorbance and the competition between product formation *via* Diels-Alder cycloaddition and deactivation *via* (E)-(Z) isomerization. In order for these effects to be practically useful in the present application, it is necessary that the ISC from the S_1 to the T_2 excited states remains feasible and that subsequent triplet HAT is—at the very least—not adversely affected by the use of electrostatic fields.

We predict that the anionic *Me*-linked CFG at position R6/R8 (the two positions are rotationally equivalent) will co-operatively deliver the optimal outcome in each of these aspects, and that these effects will be synthetically relevant even in polar solvents (**Figure 4**). While the anionic CFG at position R7 is predicted to yield the greatest ground- and excited-state effects, the resulting change in excited-state orbital character impedes the $S_0 \rightarrow T_1$ transition (Appendix §6). In DMSO, we predict that an anionic CFG at position R6/R8 can lower the energies of the $S_0 \rightarrow S_2$ and $S_0 \rightarrow T_2$ transitions by up to 88.1 kJ mol^{-1} and 27.2 kJ mol^{-1} respectively, while leaving the remaining relevant photochemistry and the triplet HAT reactivity virtually unaffected. At the same time, the competition between (*E*)-(*Z*) isomerization and Diels-Alder reactivity is now improved by an average of 7.2 kJ mol^{-1} in favour of the latter relative to the unfunctionalized *o*-alkylphenyl ketone, an enhancement that alone represents up to 80 times greater conversion from the ground state (E)-enol (*ceteris paribus*). Finally, in the Supplementary Information (Appendix §12) we briefly demonstrate with a diverse set of 19 examples that it is otherwise difficult to cooperatively promote both excited- and ground-state outcomes in the PEDA sequence using traditional substituent effects, lending further evidence towards the potentially unique synthetic utility of oriented electrostatic fields. The results of this analysis are largely consistent with the experimental yields reported by Murakami and co-workers and previous theoretical work by some of us,[26] lending support to our predictions.

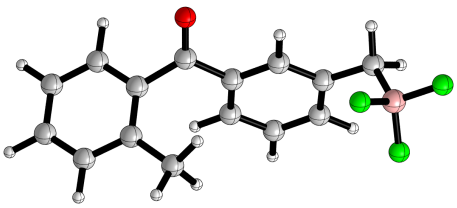

Figure 4. The CFG-modified *o*-alkylphenyl motif predicted to achieve optimal co-operative electrostatic catalysis in the ground- and excited-state.

CONCLUSION

We find that electrostatic fields arising from synthetically-accessible internal OEFs can cooperatively and selectively promote ground- and excited-state reactivity in a realistic multi-step reaction in polar solvent. Specifically, we demonstrate that OEFs can simultaneously shift the $S_0 \rightarrow S_2$ transition of *o*-alkylphenyl ketones towards the visible region while also driving product formation and CO_2 capture *via* Diels-Alder cycloaddition by selectively destabilising deactivation *via* (E)-(Z) isomerization,

with minimal compromise in excited state reactivity. Additionally, we show that the mechanism of photochemical carboxylation of *o*-alkylphenyl ketones cannot proceed *via* the mechanism suggested by Su and Su,[3] and additionally provide detailed support for the initial mechanism suggested by Murakami and co-workers.[4]

Contrary to the current understanding of electrostatic field effects, we find that the largest photochemical shifts (irrespective of position) are caused by molecular polarizability and only partially related to the distance between the CFG and the affected dipole. However, the largest individual electrostatic switches are still obtained by careful placement of spatially-close CFGs, indicating the somewhat complex relationship between electrostatic field effects and the position of the CFG relative to the affected multipoles.

Even more surprising, when polarizability is important, the role of solvent in attenuating the effects of CFGs on excited state chemistry becomes complex. On the one hand, increasing solvent polarity attenuates the resulting net transition dipole; on the other, the polarization induced by the charge is itself stabilized with increasing solvent polarity. As a result, the attenuation in the effects of CFGs with increasing solvent polarity are diminished, hence overcoming the usual trade-off between solubility and solvent polarity.

While the aim here was to drive the overall Diels-Alder/isomerization competition toward the former, we show here that (E)-(Z) bond isomerization can also be selectively targeted using electrostatic fields, and that the magnitude of effect can exceed that previously reported for Diels-Alder chemistry. These effects are readily tuned as a function of solvent choice, and/or the sign and position of the CFG, a point which has obvious implications for the future role of electrostatic fields in organic chemistry or the design of functional materials.

ASSOCIATED CONTENT

Supporting Information

The Supporting Information is available free of charge on the ACS Publications website.

AUTHOR INFORMATION

Corresponding Author

* Email: michelle.coote@anu.edu.au

Author Contributions

All authors have given approval to the final version of the manuscript.

Funding Sources

Australian Research Council (CE140100012, FL170100041)

ACKNOWLEDGMENT

The authors acknowledge financial support from the Australian Research Council (ARC) Centre of Excellence for Electromaterials Science, an ARC Laureate Fellowship (to M.L.C.), and generous supercomputing time from the National Computational Infrastructure. M.T.B acknowledges an Australian Government Research Training Program Scholarship and Dean's Merit Scholarship in Science. The authors wish to thank Vincent Doan for helpful discussions. **Figure 1** was rendered with PyMol v.2.3[35]; surfaces in **Scheme 3B** and **4B** were rendered with IQmol v.2.13[36].

REFERENCES

(1) Shaik, S.; Mandal, D.; Ramanan, R. Oriented Electric Fields as Future Smart Reagents in Chemistry. *Nat. Chem.* **2016**, *8*, 1091–1098.

(2) Shaik, S.; Ramanan, R.; Danovich, D.; Mandal, D. Structure and Reactivity/Selectivity Control by Oriented-External Electric Fields. *Chem. Soc. Rev.* **2018**, *47*, 5125–5145..

(3) Ciampi, S.; Darwish, N.; Aitken, H. M.; Díez-Pérez, I.; Coote, M. L. Harnessing Electrostatic Catalysis in Single Molecule, Electrochemical and Chemical Systems: A Rapidly Growing Experimental Tool Box. *Chem. Soc. Rev.* **2018**, *47*, 5146–5164.

(4) Stuyver, T.; Danovich, D.; Joy, J.; Shaik, S. External Electric Field Effects on Chemical Structure and Reactivity. *Wiley Interdiscip. Rev. Comput. Mol. Sci.* **2019** doi: 10.1002/wcms.1438

(5) Welborn, V. V.; Ruiz Pestana, L.; Head-Gordon, T. Computational Optimization of Electric Fields for Better Catalysis Design. *Nat. Catal.* **2018**, *1*, 649–655.

(6) Che, F.; Gray, J. T.; Ha, S.; Kruse, N.; Scott, S. L.; McEwen, J.-S. Elucidating the Roles of Electric Fields in Catalysis: A Perspective. *ACS Catal.* **2018**, *8*, 5153–5174.

(7) Klinska, M.; Smith, L. M.; Gryn'ova, G.; Banwell, M. G.; Coote, M. L. Experimental Demonstration of PH-Dependent Electrostatic Catalysis of Radical Reactions. *Chem. Sci.* **2015**, *6*, 5623–5627.

(8) Aragonès, A. C.; Haworth, N. L.; Darwish, N.; Ciampi, S.; Bloomfield, N. J.; Wallace, G. G.; Diez-Perez, I.; Coote, M. L. Electrostatic Catalysis of a Diels–Alder Reaction. *Nature* **2016**, *531*, 88–91.

(9) Akamatsu, M.; Sakai, N.; Matile, S. Electric-Field-Assisted Anion−π Catalysis. *J. Am. Chem. Soc.* **2017**, *139*, 6558–6561.

(10) Gorin, C. F.; Beh, E. S.; Bui, Q. M.; Dick, G. R.; Kanan, M. W. Interfacial Electric Field Effects on a Carbene Reaction Catalyzed by Rh Porphyrins. *J. Am. Chem. Soc.* **2013**, *135*, 11257–11265.

(11) Huang, X.; Tang, C.; Li, J.; Chen, L.-C.; Zheng, J.; Zhang, P.; Le, J.; Li, R.; Li, X.; Liu, J.; et al. Electric Field–Induced Selective Catalysis of Single-Molecule Reaction. *Sci. Adv.* **2019**, *5*, eaaw3072. doi: 10.1126/sciadv.aaw3072.

(12) Warshel, A.; Sharma, P. K.; Kato, M.; Xiang, Y.; Liu, H.; Olsson, M. H. M. Electrostatic Basis for Enzyme Catalysis. *Chem. Rev.* **2006**, *106*, 3210–3235.

(13) Fried, S. D.; Bagchi, S.; Boxer, S. G. Extreme Electric Fields Power Catalysis in the Active Site of Ketosteroid Isomerase. *Science* **2014**, *346*, 1510–1514.

(14) Pocker, Y.; Buchholz, R. F. Electrostatic Catalysis by Ionic Aggregates. II. Reversible Elimination of Hydrogen Chloride from Tert-Butyl Chloride and the Rearrangement of 1-

Phenylallyl Chloride in Lithium Perchlorate-Diethyl Ether Solutions. *J. Am. Chem. Soc.* **1970**, *92*, 4033–4038.
(15) Smith, P. J.; Wilcox, C. S. The Intramolecular Salt Effect. *The J. Org. Chem.* **1990**, *55*, 5675–5678.
(16) Smith, P. J.; Wilcox, C. S. The Chemistry of Functional Group Arrays. Electrostatic Catalysis and the "Intramolecular Salt Effect". *Tetrahedron* **1991**, *47*, 2617–2628.
(17) Raposo, C.; Wilcox, C. S. The Intramolecular Salt Effect in Chiral Auxiliaries. Enhanced Diastereoselectivity in a Nitrile Oxide Cycloaddition via Rational Transition State Stabilization. *Tetrahedron Lett.* **1999**, *40*, 1285–1288.
(18) Hill, N. S.; Coote, M. L. Internal Oriented Electric Fields as a Strategy for Selectively Modifying Photochemical Reactivity. *J. Am. Chem. Soc.* **2018**, *140*, 17800–17804.
(19) Hill, N. S.; Coote, M. L. Strategies for Red-Shifting Type I Photoinitiators: Internal Electric Fields versus Lewis Acids versus Increasing Conjugation. *Aust. J. Chem.* **2019**, *72*, 627.
(20) Blyth, M. T.; Coote, M. L. A PH-Switchable Electrostatic Catalyst for the Diels–Alder Reaction: Progress toward Synthetically Viable Electrostatic Catalysis. *J. Org. Chem.* **2019**, *84*, 1517–1522.
(21) Aitken, H. M.; Coote, M. L. Can Electrostatic Catalysis of Diels–Alder Reactions Be Harnessed with PH-Switchable Charged Functional Groups? *Phys. Che, Chem. Phys.* **2018**, *20*, 10671–10676.
(22) Masuda, Y.; Ishida, N.; Murakami, M. Light-Driven Carboxylation of o-Alkylphenyl Ketones with CO2. *J. Am. Chem. Soc.* **2015**, *137*, 14063–14066.
(23) Yang, N. C.; Rivas, C. A New Photochemical Primary Process, the Photochemical Enolization of o-Substituted Benzophenones. *J. Am. Chem. Soc.* **1961**, *83*, 2213–2213.
(24) Su, S.-H.; Su, M.-D. Mechanistic Analysis of the Photochemical Carboxylation of O-Alkylphenyl Ketones with Carbon Dioxide. *RSC Adv.* **2016**, *6*, 50825–50832.
(25) Frisch, M. J.; Trucks, G. W.; Schlegel, H. B.; Scuseria, G. E.; Robb, M. A.; Cheeseman, J. R.; Scalmani, G.; Barone, V.; Petersson, G. A.; Nakatsuji, H.; et al. *Gaussian 16, Revision A.03*; Gaussian, Inc.: Wallingford CT, 2016.
(26) Menzel, J. P.; Noble, B. B.; Lauer, A.; Coote, M. L.; Blinco, J. P.; Barner-Kowollik, C. Wavelength Dependence of Light-Induced Cycloadditions. *J. Am. Chem. Soc.* **2017**, *139*, 15812–15820.
(27) Zhao, Y.; Truhlar, D. G. The M06 Suite of Density Functionals for Main Group Thermochemistry, Thermochemical Kinetics, Noncovalent Interactions, Excited States, and Transition Elements: Two New Functionals and Systematic Testing of Four M06-Class Functionals and 12 Other Functionals. *Theor. Chem. Acc.* **2008**, *120*, 215–241.
(28) Marenich, A. V.; Cramer, C. J.; Truhlar, D. G. Universal Solvation Model Based on Solute Electron Density and on a Continuum Model of the Solvent Defined by the Bulk Dielectric Constant and Atomic Surface Tensions. *J. Phys. Chem. B* **2009**, *113* 6378–6396.
(29) Ho, J.; Klamt, A.; Coote, M. L. Comment on the Correct Use of Continuum Solvent Models. *J. Phys. Chem. A* **2010**, *114*, 13442–13444.
(30) Gryn'ova, G.; Coote, M. L. Origin and Scope of Long-Range Stabilizing Interactions and Associated SOMO–HOMO Conversion in Distonic Radical Anions. *J. Am. Chem. Soc.* **2013**, *135*, 15392–15403.
(31) Meir, R.; Chen, H.; Lai, W.; Shaik, S. Oriented Electric Fields Accelerate Diels–Alder Reactions and Control the Endo/Exo Selectivity. *ChemPhysChem* **2010**, *11*, 301–310.
(32) Zang, Y.; Zou, Q.; Fu, T.; Ng, F.; Fowler, B.; Yang, J.; Li, H.; Steigerwald, M. L.; Nuckolls, C.; Venkataraman, L. Directing Isomerization Reactions of Cumulenes with Electric Fields. *Nat Commun* **2019**, *10*, 1–7.
(33) Gryn'ova, G.; Coote, M. L. Directionality and the Role of Polarization in Electric Field Effects on Radical Stability. *Aust. J. Chem.* **2017**, *70*, 367-372.
(34) Salem, L.; Stohrer, W.-D. A Double-Well Potential for Olefin Isomerization in Polar Solvents. *J. Chem. Soc., Chem. Commun.* **1975**, 5, 140–142.
(35) Schrödinger, L. *PyMOL Molecular Graphics System*; Schrödinger, LLC., 2019.
(36) Gilbert, A. *IQmol*; 2019.

Table of Contents Graphic